HHS Public Access

Cannabinoid receptor 2 mediates retention of immature B cells in bone marrow sinusoids

João P. Pereira[1], **Jinping An**[1], **Ying Xu**[1], **Yong Huang**[2], and **Jason G. Cyster**[1]

[1]Howard Hughes Medical Institute and Department of Microbiology and Immunology, University of California San Francisco, CA 94143, USA

[2]Drug Studies Unit, Department of Biopharmaceutical Sciences, University of California San Francisco, 347 Littlefield Ave, South San Francisco, CA-94080, USA

Abstract

Immature B-cells developing in the bone marrow (BM) are found in parenchyma and sinusoids. The mechanisms controlling B-cell positioning within sinusoids are not understood. Here we showed that integrin $\alpha_4\beta_1$ and VCAM-1 are required, whereas CXCR4 is dispensable for sinusoidal retention. Instead, cannabinoid receptor 2 (CB2), a $G\alpha_i$-coupled receptor upregulated in immature B-cells, was required for sinusoidal retention. Using two-photon microscopy, we observed immature B-cells entering and crawling within sinusoids; these immature B-cells were displaced by CB2 antagonism. Moreover, CB2-deficient mice contain a reduced frequency of λ^+ B-cells in the peripheral blood and spleen. Our findings identify unique requirements for B-cell retention in the BM sinusoidal niche, and suggest a role for CB2 in B-cell repertoire generation.

Introduction

The bone marrow (BM) contains specialized, yet poorly defined, microenvironments that help maintain stem cells and support hematopoiesis. In early studies examining the compartmentalization of developing B-cells, B220$^+$ cells and immature IgM$^+$ cells were found scattered throughout the BM parenchyma, and immature IgM$^+$ cells were also observed inside sinusoids 1-4. BM sinusoids are specialized thin walled venous blood vessels that travel through the tissue parenchyma, often anastamosing before connecting to the large central sinusoid that carries the blood and newly produced cells to venous circulation 5. All the cells produced in the BM, including red blood cells, platelets, granulocytes and lymphocytes, are thought to enter circulation via sinusoids 5. Given this cellular diversity, lymphocytes were unexpectedly enriched within sinusoids, and it was suggested that there might be 'lymphocyte loading' of sinusoids 2, 6. However, the mechanisms controlling immature B-cell retention in or release from BM sinusoids have not been defined.

Correspondence should be addressed to J.G.C, (Jason.Cyster@ucsf.edu).

The integrin-ligand pair $\alpha_4\beta_1$-VCAM-1 helps retain hematopoietic stem cells in the BM 7-9. VCAM-1 is expressed by a subset of BM stromal cells and by sinusoidal endothelium 9. The role of $\alpha_4\beta_1$-VCAM-1 interactions in B-cell development or retention within the BM has been unclear, as some gene ablation studies suggested a minimal role 10-13 whereas others documented a reduction in immature and mature B-cells in the BM 14, 15. SDF-1 (also called CXCL12), a chemokine that can activate $\alpha_4\beta_1$ 16, is produced by BM stromal cells and has also been detected on BM endothelium 17-19. The SDF-1 receptor, CXCR4, helps retain hematopoietic progenitor cells and developing B-cells in the BM 20, 21 and promotes homing of progenitor cells, plasma cells and T cells from blood to BM 19, 22, 23. However, CXCR4 is partially downregulated between the pre-B and immature B-cell stages 16, 21, 24-26, and it is unclear whether CXCR4 continues to function in immature B-cells.

The $G\alpha_i$-coupled cannabinoid receptor-2 (CB2) is abundantly expressed in mature B-cells and is also present in myeloid cells, natural killer (NK) cells and various other cell types 27, 28. The CB2 ligand, 2-arachidonoylglycerol (2-AG), is generated from arachidonic acid-containing phospholipids and has been detected in many tissues including bone 28, 29. Intake of cannabinoid receptor agonists has a variety of effects on the immune system but the direct *in vivo* actions on lymphoid cells remain poorly understood 30.

Here we use an *in vivo* pulse labeling procedure to distinguish cells inside BM sinusoids from those in the parenchyma, and to establish that immature B-cell retention in sinusoids is dependent on $\alpha_4\beta_1$ and VCAM-1. CXCR4 is not critical for retention in sinusoids but pertussis toxin-mediated inhibition of $G\alpha_i$ displaces sinusoidal cells. CB2 expression and function is upregulated in immature B-cells and intrinsic deficiency in CB2 prevents immature B-cell accumulation in BM sinusoids. By two-photon microscopy we observed immature B-cells entering and crawling within BM sinusoids; these cells were displaced by CB2 antagonism. Finally, CB2-deficiency caused a reduction in the percent of peripheral B-cells expressing Igλ. Our findings identify unique requirements for B-cell retention in the BM sinusoidal niche, and establish a role for CB2 in formation of the B-cell repertoire.

Results

Labeling of cells in BM sinusoids

To examine the distribution of IgM$^+$ B-cells between BM parenchyma and sinusoids we stained BM sections for endothelial and basement membrane markers. Antibodies against laminin, a protein abundant in basement membranes, were effective in labeling BM vessels; sinusoids were identified amongst laminin-expressing vessels based on their large lumens and thin walls (Fig. 1a). IgM$^+$ B-cells in the femur and tibia were detected both in the parenchyma and inside sinusoids (Fig. 1a), consistent with earlier studies 1, 4.

To facilitate quantification and phenotyping of sinusoidal B-cells, an *in vivo* labeling procedure was developed. Previous studies showed that injected antibodies rapidly equilibrated throughout the BM 1, 4, 5 and we found that biotin-conjugated CD19-specific antibodies labeled all BM B-cells within a few minutes of injection (Supplementary Fig. 1, online). To test the possibility that larger protein complexes may have more limited access to the parenchyma, we treated mice for 2 minutes with anti-CD19 (approximately 150kD)

that had been coupled to phycoerythrin (PE, 240kD). In this case, a bimodal staining pattern was observed amongst immature IgM^+IgD^- and IgM^+IgD^{lo} B-cells and mature B-cells; in contrast pro- and pre-B-cells were unlabeled (Fig. 1b). Amongst the IgM^+ immature B-cells the IgD^{lo} subset was most enriched for anti-CD19-PE labeled cells (Fig. 1b). Injection of PE-conjugated antibodies for longer periods (5–10 minutes) eventually stained all BM cells targeted by the antibodies (Supplementary Fig. 1). When immature B-cells were analyzed with a single gate (encompassing IgM^+IgD^- and IgM^+IgD^{lo} cells – Supplementary Fig. 1), 25.4±5.9% (n=18) were labeled with anti-CD19-PE. The extent of staining on the brightly labeled BM B-cell subsets approached the labeling intensity of cells from blood of the same animals (Fig. 1c). Immunofluorescence analysis of BM sections from mice treated with anti-CD19-PE, once stained with anti-laminin, revealed that the CD19-PE-labeled cells were within sinusoids (Fig. 1d and Supplementary Fig. 2, online). However, *in vitro* staining with anti-CD19-PE showed the expected distribution of $CD19^+$ cells in both the parenchyma and within sinusoids (Fig. 1d and Supplementary Fig. 2). In some cases the *in vivo* labeled cells were located in regions of sinusoids adjoining the central collecting sinusoid (Supplementary Fig. 2).

Using anti-CD45-PE injection as an approach to label all hematopoietic cell types present within sinusoids, we found that B lineage cells constituted approximately two-thirds of all sinusoidal cells and the remaining cells were mostly of myeloid lineage ($CD11b^+$, $CD11c^+$ and/or $Gr1^+$), together with smaller numbers of NK cells ($NK1.1^+$) and $CD4^+$ and $CD8^+$ T cells (Fig. 1e). The proportion of immature B-cells labeled following anti-CD45-PE injection was similar to that found in mice treated with anti-CD19-PE (data not shown). Consistent with the flow cytometry data, analysis of BM sections from mice treated with anti-CD19-PE and stained *in vitro* with anti-CD45 showed that B-cells were the predominant $CD45^+$ cell type within sinsuoids (Fig. 1f). In summary, treatment with PE-conjugated antibodies *in vivo* for 2 minutes allowed selective labeling of cells present within BM sinusoids and this approach revealed that about one quarter of immature B-cells in the BM are located within this BM niche.

$\alpha_4\beta_1$ and VCAM-1 retain sinusoidal B-cells

To test whether $\alpha_4\beta_1$ and VCAM-1 were involved in retaining immature B-cells inside BM sinusoids, mice were treated with blocking antibodies against α_4 or VCAM-1, or with saline for 3 h, and injected with anti-CD19-PE two minutes prior to tissue isolation. A separate group of mice was treated with anti-α_L to block $\alpha_L\beta_2$ (also called LFA-1). Enumeration of parenchymal (anti-CD19-PE$^-$) B lineage cells showed that immature IgD^- and IgD^{lo} cells were slightly, but significantly, reduced in mice treated with α_4 blocking antibodies, whereas in anti-α_L treated mice the numbers remained unchanged (Fig. 2a). Mature B-cells were also reduced by anti-α_4 and anti-VCAM-1, but not anti-α_L treatment (Fig. 2a). In contrast to these mild effects, we found a marked reduction of immature B-cells inside the sinusoids (anti-CD19-PE$^+$) of mice treated with α_4 or VCAM-1 blocking antibodies (Fig. 2b). The number of sinusoidal mature B-cells was also reduced. However, anti-α_L treatment did not result in significant changes in the number of sinusoidal B-cells (Fig. 2b). Enumeration of IgM^+ cells within frozen sections confirmed the displacement of B-cells from BM sinusoids following α_4 blockade (Supplementary Fig. 3, online). Release of cells

from BM sinusoids of mice treated with α_4 or VCAM-1 blocking antibodies was reflected in a significant increase in the numbers of the same B-cell subsets in the peripheral blood (Supplementary Fig. 3). Some pro- and pre-B-cells were also detected in the blood, often appearing prominent compared to their absence in control blood; however, consistent with the BM enumeration data their absolute numbers were at least an order of magnitude lower than the numbers of immature B-cells. Blocking P-selectin, or P- and E-selectins, for three hours did not result in significant changes in the number of B-cells inside BM sinusoids (data not shown).

Immature B-cells in the BM parenchyma and sinusoids can be distinguished from those in the blood by higher expression of CD93 (AA4.1) on the cell surface (Fig. 2c). Notably, the immature B-cells found in blood after anti-α_4 treatment resembled those in the BM with regard to CD93 expression (Fig. 2c). This finding is consistent with the conclusion that the increase in blood immature B-cells was due to release of cells from the BM. The CD93 staining data also highlighted the phenotypic similarity of the BM parenchymal and sinusoidal immature B-cell populations (Supplementary Fig. 1).

To test the role of the β_1 integrin chain in B-cell retention within sinusoids, we crossed mice bearing loxP sites flanking *Itgb1* 31 with mice that express Cre from the *Cd19* locus 32. In *Itgb1$^{f/f}$Cd19*$^{Cre/+}$ mice, the proportion of B-cells that underwent *Igtb1* deletion (identified by lack of surface β_1 staining) increased gradually during B-cell development (Fig. 3a), consistent with on-going Cre-mediated deletion 33. Pulse labeling with anti-CD45-PE revealed that in *Itgb1$^{f/+}$Cd19*$^{Cre/+}$ and *Itgb1$^{f/f}$Cd19*$^{Cre/+}$ mice there was a strong bias against β_1-deficient immature B-cells within the sinusoidal CD45$^+$ compartment (Fig. 3a, b). In contrast, peripheral blood was enriched with immature B-cells that had lost β_1 expression, consistent with the notion that β_1 promotes retention of these cells in the BM (Fig. 3c). Analysis of mature B-cells was problematic because on this subset β_1-surface staining did not allow a clear distinction between cells expressing and lacking β_1 (data not shown). Taken together, these findings indicate that $\alpha_4\beta_1$ and VCAM-1 are required for the retention of immature B-cells and mature recirculating B-cells inside BM sinusoids.

Retention in parenchyma requires CXCR4

Cxcr4 transcripts are abundant in pre-B-cells and decrease by more than 4-fold in immature IgD$^-$ and IgD^{lo} cells (Fig. 4a). Using Cd19-Cre to ablate *Cxcr4* in developing B-cells we found that an increased fraction of CXCR4-deficient immature BM B-cells, and nearly all CXCR4-deficient mature BM B-cells, were located inside sinusoids (Fig. 4b,c). Cells that had not yet undergone Cre-mediated loss of *Cxcr4* expression remained normally partitioned between parenchyma and sinusoids, establishing that the effect of *Cxcr4* ablation was cell intrinsic (Fig. 4b,c). The incomplete *Cxcr4* ablation in *Cxcr4$^{f/f}$Cd19*$^{Cre/+}$ mice made it problematic to determine the impact on total BM cell numbers, but there was a trend toward reduced numbers of immature IgD^{lo} B-cells and a significant reduction in mature B-cells (Fig. 4c). When CXCR4 was globally inhibited in wild-type mice by 2 h treatment with the CXCR4 antagonist 4F-benzoyl TN14003 34 the frequency and number of immature IgD^{lo} and mature B-cells was significantly reduced in the BM parenchyma and increased inside sinusoids (Fig. 4d). The cells accumulating in sinusoids following TN14003 treatment

could, however, be released by α_4 integrin blockade, leading to their increased representation in peripheral blood (Fig. 4e). These findings suggest that immature B-cells, especially the IgD^{lo} subset, are retained in the BM parenchyma in a CXCR4-dependent manner, but that alternative retention mechanism(s) operate to promote integrin-mediated retention inside BM sinusoids.

As integrin activity within lymphoid cells is typically induced by $G\alpha_i$-coupled receptors, we tested the impact of inhibiting all $G\alpha_i$ function using PTX. When mice were treated with PTX for one day there was marked displacement of immature IgM$^+$IgD^{lo} B-cells from BM sinusoids (Fig. 4f). These observations suggested the involvement of additional $G\alpha_i$-coupled receptor(s) in promoting immature B-cell retention in the sinusoidal niche.

CB2 retains immature B-cells in sinusoids

A comparison of G-protein coupled receptor transcript abundance in pre-B and immature B-cells using Affymetrix gene array data (accession code GDS52)35 revealed increased expression of *Cnr2* mRNA transcripts, which encode CB2, in immature B-cells; a 2-fold increase was confirmed by qRT-PCR (Fig. 5a). In migration assays, immature B-cells responded more strongly to the CB2 ligand 2-AG than pro-B or pre-B-cells (data not shown), and amongst the immature cells, the response was greatest for the sinusoidal subpopulation (Fig. 5b). CB2-deficient mice showed normal numbers of developing BM B-cells but exhibited a dearth of immature B-cells within sinusoids (Fig. 5c). However, CB2-deficient cells were over-represented amongst immature B-cells in blood, consistent with defective retention in sinusoids (Fig. 5c). The total number of mature follicular B-cells in blood (Fig. 5c) and spleen (data not shown) was not affected by CB2-deficiency. Analysis of mixed BM chimeras showed that the CB2 requirement for sinusoidal localization of immature (and mature) BM B-cells was cell intrinsic (Fig. 5d). By mass spectrometry analysis, the CB2 ligand 2-AG was detected in low amounts in plasma and in high amounts in BM, as well as in the spleen and brain (Fig. 5e). Finally, transfers of activated B-cells transduced with a retrovirus encoding CB2 showed that increased expression of CB2 favored sinusoidal over parenchymal lodgment of transferred cells (Fig. 5f). These findings demonstrate that CB2 has high activity within sinusoidal B-cells and is required for their efficient lodgment in BM sinusoids.

Dynamic behavior of sinusoidal B-cells

To examine the migration dynamics of immature B-cells within sinusoids we performed intravital two-photon microscopy of $Rag1^{GFP/+}$ cells in BM within the mouse calvarium. These mice contain a GFP cassette knocked into one $Rag1$ allele. As expected, GFP was detected by flow cytometry in $Rag1^{GFP/+}$ pro-B-cells and more abundantly in pre-B and immature B-cells whereas most mature B-cells did not express GFP (Fig. 6a)36. Using *in vivo* CD19-PE labeling we confirmed that the immature IgM$^+$IgD$^-$ and IgM$^+$IgD^{lo} B-cells inside sinusoids were GFP^{hi} (Fig. 6a) and, reciprocally, that more than 94% of the GFP^{hi} sinusoidal B-cells expressed CD93 (Fig. 6b).

Using dextran-rhodamine to distinguish sinusoids and other blood vessels from BM parenchyma, numerous GFP$^+$ cells were identified in the parenchyma, most likely

corresponding to pre-B and immature B-cells; a fraction of these cells were motile (Fig. 6c and Supplementary Movies 1 and 2, online), some with median velocities of 4-7 μm/min (Fig. 6d). Many of the cells showing median velocities of 2-4 μm/min corresponded to cells that extended processes but exhibited little displacement above the background movement of the tissue. Importantly, GFP+ cells were also observed within vessels and though many were poorly motile, some were migrating in various directions (Fig. 6e and Supplementary Movies 1 and 2) at median velocities ranging from 5 to 10 μm/min (Fig. 6d). Although only small numbers of newly generated B-cells are expected to migrate from the parenchyma into sinusoids during 30-60 min imaging periods, we did observe several examples of GFP+ cells entering sinusoids (Fig. 6e and Supplementary Movie 1). Notably, after entry these cells remained adherent and in some cases the cells continued migrating. Occasionally, a cell in flow within the sinusoid was observed to become adherent and begin crawling (Fig. 6f and Supplementary Movie 2). GFP+ cells could also be detected detaching and being rapidly carried away with the blood flow (Supplementary Movie 2). GFP− cells were observed as dark halos within the dextran-rhodamine labeled sinusoids and they often moved bidirectionally within a given vessel (Supplementary Movies 1 and 2).

Consistent with most immature sinusoidal B-cells having recently entered from the BM parenchyma, BrdU labeling experiments showed that sinusoidal B-cells were replaced by newly generated cells with only a slight lag compared to parenchymal B-cells and more rapidly than immature B-cells in the blood (Supplementary Fig. 4, online).

To further characterize how CB2 promotes cell lodgment within sinusoids we asked whether cells were continuously dependent on CB2 signaling by testing the effect of treatment with a CB2 antagonist, SR144528 37. A 3 h treatment with this molecule led to a marked displacement of sinusoidal B-cells and had no affect on parenchymal cells (Fig. 7a). Immature B-cell numbers were correspondingly increased in the blood of treated mice (Fig. 7a). Intravital imaging 90-240 min after SR144528 treatment showed a greater number of flowing GFP+ cells than in the period prior to antagonist treatment (Fig. 7b). Reciprocally, in an *in vitro* assay, incubation of BM cells with 2-AG increased the adhesion of sinusoidal B-cells to a VCAM-1-coated surface under shear (Fig. 7c). Taken together, these experiments suggest that CB2 promotes adhesion of immature B-cells within BM sinusoids.

Reduced Igλ+ B-cell frequency

As an approach to test the influence of CB2 on B-cell repertoire development we examined the frequency of Igκ+ and Igλ+ B-cells in CB2-deficient mice. CB2-deficiency led to a reduction in the frequency of Igλ+ immature and mature B-cells in the blood and spleen (Fig. 8a). Similar findings were obtained in mixed BM chimeras (Fig. 8b). Treatment of wild-type mice with the CB2 antagonist for 6-9 days also led to a reduction in Igλ+ B-cell frequencies amongst immature splenic B-cells (Fig. 8c). These observations provide evidence of a B-cell intrinsic role for CB2 in establishing the peripheral B-cell repertoire.

Discussion

In the above work we demonstrate that approximately one quarter of the immature B-cells in mouse BM are situated inside sinusoids. The cells migrate within this compartment, and

their retention is dependent on $\alpha_4\beta_1$–VCAM-1 interactions and on the $G\alpha_i$-coupled CB2 receptor. The presence of large numbers of adherent and migrating immature B-cells inside sinusoids suggests that rather than serving solely to support blood flow, these vessels constitute a specialized cellular niche within the BM that may influence B-cell development. In support of such a role, CB2-deficiency led to a reduction in the frequency of Igλ^+ immature and mature B-cells in the periphery.

CB2 is abundantly expressed in B-lymphocytes and *in vitro* studies have described peripheral B-cell migration in response to 2-AG [38, 39]. Marginal zone B-cell numbers are reduced in the absence of CB2, though whether CB2 is acting to promote marginal zone B-cell development, retention or survival remains unclear [40]. Our studies suggest that CB2 promotes $\alpha_4\beta_1$-mediated adhesion of B-cells to sinusoidal endothelial cells. In addition to $G\alpha_i$-signaling [16] exposure to shear conditions promotes integrin adhesive function [41]. Thus CB2 signaling and shear may work together to promote $\alpha_4\beta_1$–VCAM-1-mediated adhesion in BM sinusoids. Although we believe this is the most parsimonious interpretation of our data, we cannot exclude that the in vivo actions of $\alpha_4\beta_1$ and CB2 are independent and that CB2 acts by some other mechanism to promote cell positioning in sinusoids. 2-AG can be made by many cell types [28], although given the multiple 2-AG biosynthetic pathways it will take new tools and approaches to determine whether endothelial cells or other BM cell types are the relevant source of this lipid. It is notable that immature B-cells from sinusoids are more responsive to 2-AG than are parenchymal cells, suggesting a change in CB2 receptor function occurs as immature B-cells enter, or commit to entering, the vascular compartment.

Development of Igλ^+ B-cells is delayed by several hours compared to Igκ^+ cells and many Igλ^+ cells show evidence of receptor editing at the *Igk* locus [42, 43]. Studies in Ig transgenic systems have shown that the frequency of Igλ^+ B-cells correlates with the extent of receptor editing [44]. We speculated that by reducing total time spent within the BM, CB2-deficiency might diminish the time available for receptor editing and thus the frequency of Igλ^+ B-cells. The reduced frequency of Igλ^+ B-cells amongst immature blood and splenic B-cells at first seemed consistent with this scenario. However, our inability to detect a reduction in Igλ^+ B-cell frequencies in the BM suggests CB2-deficiency affects processes acting after Igλ rearrangement. We propose that the reduced immature B-cell retention time in sinusoids increases the likelihood of Igλ^+ B-cell loss during or shortly after their release in to the periphery. It is notable that there is a reduction in Igλ^+ B-cell frequency in the mature compared to immature splenic B-cell compartment of wild-type mice, suggesting that Igλ^+ cells are prone to negative selection following release from the BM. CB2–deficiency and disrupted occupancy of the BM sinusoidal niche may exaggerate this effect. It is possible that CB2 deficiency also causes loss of B-cells bearing certain *Igk* rearrangements and it will be valuable to analyze the diversity of the Igκ repertoire in future studies. While our data are consistent with the altered peripheral B-cell repertoire being a consequence of the sinusoidal CB2 role, we cannot currently exclude that it is also due to a peripheral function of this receptor. Treatment with agonists of cannabinoid receptors can lead to alterations in antibody responses [30, 45, 46]. The role of CB2 in B-cell repertoire formation may contribute to these altered responses.

Previous work suggested a lack of effect on B-cell development in adult mice in which integrin-α_4 or integrin-β_1 were conditionally ablated[10-12] whereas other reports have shown a selective reduction in immature B-cell numbers in the BM following conditional VCAM-1 ablation [14, 15]. Our findings are in agreement with the latter studies, and further indicate that the cells most dependent on $\alpha_4\beta_1$-VCAM-1 mediated adhesion are cells located within BM sinusoids. Moreover, we provided evidence that $\alpha_4\beta_1$ adhesive activity may be promoted by ligand engagement of CB2.

By intravital imaging we observed that the parenchymal *Rag1*-expressing B-cell population is made up both of sessile and migratory cells. Examination of cell distribution in static images of BM showed repositioning occurred between pro-B and pre-B-cell stages [47] making it likely that some of the migrating parenchymal cells are pre-B-cells. We speculate that many immature B-cells are also motile, perhaps surveying for autoantigens or sites of entry to sinusoids. Previous studies with transferred cells showed that mature B-cells are able to migrate within the BM parenchyma, although the fraction of cells migrating and the migration velocities were not determined [48]. Within sinusoids the Rag1-GFP label was specific for immature B-cells, allowing us to conclude that sinusoidal immature B-cells include both actively migrating and poorly motile cells. The purpose of the B-cell motility is not yet clear but it may facilitate encounter with sinusoidal self-antigens. Our detection of immature B-cells entering and then crawling within BM sinusoids establishes that at least some of the sinusoidal B-cells are cells that recently entered the structures. Our data indicates that immature B-cells may also sometimes transition from a flowing, non-adherent state to an adherent state. Video microscopy of sinusoids within rabbit tibia revealed alternate movement and stagnation in the blood flow [5]. Irregularly shaped sinusoids with unpredictable fluctuations in blood flow have also been observed in earlier studies of mouse frontoparietal skull BM [8]. It seems likely that with these unusual blood flow characteristics cells that detach may frequently re-encounter the sinusoidal wall rather than being immediately flushed from the marrow, providing additional opportunities for $\alpha_4\beta_1$-VCAM-1 and CB2-mediated retention.

CXCR4 and SDF-1 play many roles within the BM, including the induction of cell adhesion to blood vessels [18, 23]. It was therefore surprising that CXCR4 antagonism failed to displace immature B-cells from sinusoids. This finding might be considered consistent with evidence from static adhesion assays that CXCR4 is ineffective in promoting sustained adhesion of immature B-cells [16]. In contrast, the quantitatively greater release of IgM$^+$IgD^{lo} immature (and mature) B-cells than pro-B or pre-B-cells from the BM parenchyma after CXCR4 blockade suggests that immature B-cells are particularly dependent on CXCR4 for retention in the parenchyma. We propose that pro-B and pre-B-cells have additional retention systems that keep them within the BM parenchyma. Reciprocally, immature B-cells may have increased expression of receptors that respond to egress promoting cues or molecules that facilitate motility and transendothelial migration. Despite the importance of CB2 in promoting retention of immature B-cells within BM sinusoids, we did not detect immature B-cell accumulation in the parenchyma of CB2-deficient mice arguing against an essential role for this receptor in promoting sinusoid entry, although a redundant contribution of CB2 to this step is not excluded.

Intravascular lymphoma is a condition where malignant B-cells accumulate inside blood vessels, sometimes including BM sinusoids [49]. The BM is also a site of tumor metastasis, and SDF-1 has been implicated in promoting adhesion of malignant cells in BM blood vessels [18]. Future studies are needed to determine if CB2 and 2-AG also promote lymphoma and tumor cell adhesion in BM sinusoids.

Methods

Mice

Adult C57Bl/6 (Ly5.2$^+$) mice aged 6-8 weeks were either from The Jackson Laboratories or from the National Cancer Institute, and adult Boy/J (Ly5.1$^+$; stock no. 002014) mice were from The Jackson Laboratories. *Cnr2$^{-/-}$* mice (stock no. 005786; The Jackson Laboratories) were backcrossed to C57Bl/6 for 7-10 generations. *Cxcr4$^{+/-}$* mice [50] were crossed to *Cxcr4$^{f/f}$* [21] and to *Cd19$^{Cre/+}$* mice[32] to generate *Cxcr4$^{f/-}$ Cd19$^{Cre/+}$* and control littermates. *Itgb1$^{f/f}$* mice[31] (stock no. 004605; The Jackson Laboratories) were crossed to *Cd19$^{Cre/+}$* mice to generate *Itgb1$^{f/f}$* mice expressing a single Cd19-Cre allele, or further intercrossed to obtain *Itgb1$^{f/f}$* mice expressing two Cd19-Cre alleles and control littermates. *Rag1$^{GFP/+}$* mice[36] were provided by T. Gerdes and M. Wabl (UCSF). For generation of BM chimeras, approximately 1.5×10^6 total BM cells from either *Cnr2$^{+/+}$* or *Cnr2$^{-/-}$* (Ly5.2$^+$) mice were mixed with 1.5×10^6 total BM cells from adult Boy/J (Ly5.1$^+$) mice and transferred into adult Boy/J mice that had been exposed to two rounds of 550 Rad separated by 3 h. Chimeras were analyzed at least 6 weeks after reconstitution. Intravital two-photon microscopy and BrdU labeling was as detailed in Supplementary Methods.

Labeling of sinusoidal cell populations

Labeling of sinusoidal cells was performed by injecting mice i.v. with 1μg of PE conjugated rat anti-mouse CD19 (clone 1D3, BD Biosciences) or mouse anti-mouse CD45.2 (Ly5.2-PE, clone 104, BD Biosciences) in 200uL of PBS for 2 min unless otherwise indicated. Mice were then immediately euthanized in a CO_2 chamber, and tissue prepared as described above. In some experiments, mice were injected with varying doses of biotin conjugated rat-anti-mouse CD19 (clone 1D3, BD Biosciences). BM cells from mutant and control mice were then stained with anti-IgD-FITC, anti-IgM-PECy7, anti-CD19- PECy5.5 (Invitrogen), anti-AA4.1-APC, and biotinylated anti-CXCR4 or unconjugated anti-Itgb1 (clone MB1.2, Chemicon International) and biotin-SP-AffiniPure F(ab′)$_2$ Fragment Goat Anti-Rat IgG, Fcγ fragment specific (Jackson Immunoresearch), followed by streptavidin QD605 (Molecular Probes). In vivo integrin, VCAM-1, selectin, CXCR4 and CB2 blocking protocols are detailed in Supplementary Methods. Cell sorting, chemotaxis and adhesion assay details are also included in Supplementary Methods. In vivo integrin, VCAM-1, selectin, CXCR4 and CB2 blocking protocols are included in Supplementary Methods. Cell sorting, chemotaxis and adhesion assay details are also included in Supplementary Methods.

Histology

Femurs and tibias were placed in Tissue Tek Optimum Cutting Temperature (OCT) compound (Sakura) and immediately frozen using a mixture of ethanol and dry ice, and stored at −80°C. 7μm cryostat sections were transferred to CJ1X adhesive coated slide using

the Cryojane® Tape Transfer System (Instrumedics) according to the manufacturer's protocol. Slides were acetone fixed, incubated with rabbit anti-mouse laminin (Sigma) and rat anti-mouse IgD (biotinylated clone 11-28 from Southern Biotechnology) followed by horse raddish peroxidase conjugated goat anti-rabbit IgG, and alkaline phosphatase conjugated goat anti-rat IgG (both from Jackson ImmunoResearch), developed, mounted and images collected as described 22. For immunofluorescence, unfixed anti-laminin stained slides were incubated with goat anti-rabbit IgG AMCA (Jackson Immunoresearch) and analyzed in an inverted fluorescent microscope (Axiovert 200M; Carl Zeiss MicroImaging, Inc.) using a plan-Neofluar 40× oil immersion objective (NA 1.3; Carl Zeiss MicroImaging, Inc.), or in an inverted fluorescent microscope (Zeiss). Images were captured with a CCD SensiCam (PCD; Cooke Corp.) and analyzed with SlideBook software (Intelligent Imaging).

Mass spectrometry

2-AG was analyzed using Micromass Quattro Ultima LC/MS/MS system with electrospray/ positive ionization mode. The Multiple Reaction Monitor (MRM) was set at 379.2 > 287.2 m/z for 2-AG and 387.4>294.5 m/z for 2-AG-d8 (Cayman Chemicals) as internal standard (IS). The cone voltage and collision energy were set as 35 V and 16 eV, respectively. The column was Synergi Polar RP (75 mm × 4.6 mm, 4 mm particle size) with mobile phase consisting of 68% acetonitrile containing 0.1 % formic acid. The flow rate was 1.0 ml/min with ¼ split into the mass system.

Supplementary Material

Refer to Web version on PubMed Central for supplementary material.

Acknowledgments

References

1. Batten SJ, Osmond DG. The localization of B lymphocytes in mouse bone marrow: radioautographic studies after in vivo perfusion of radiolabelled anti-IgM antibody. J Immunol Methods. 1984; 72:381–399. [PubMed: 6332152]

2. Osmond DG, Batten SJ. Genesis of B lymphocytes in the bone marrow: extravascular and intravascular localization of surface IgM-bearing cells in mouse bone marrow detected by electron-microscope radioautography after in vivo perfusion of 125I anti-IgM antibody. Am J Anat. 1984; 170:349–365. [PubMed: 6383003]

3. Hermans MH, Hartsuiker H, Opstelten D. An in situ study of B-lymphocytopoiesis in rat bone marrow. Topographical arrangement of terminal deoxynucleotidyl transferase-positive cells and pre-B cells. J Immunol. 1989; 142:67–73. [PubMed: 2491874]

4. Jacobsen K, Osmond DG. Microenvironmental organization and stromal cell associations of B lymphocyte precursor cells in mouse bone marrow. Eur J Immunol. 1990; 20:2395–2404. [PubMed: 2253679]

5. Tavassoli, M.; Yoffey, JM. Marrow Circulation. In: Liss, Alan R., editor. Bone Marrow Structure and Function 1-300. New York: 1983. p. 1-300.

6. Yoffey JM, Hudson G, Osmond DG. The lymphocyte in guinea-pig bone marrow. J Anat. 1965; 99:841–860. [PubMed: 5867171]

7. Jacobsen K, Kravitz J, Kincade PW, Osmond DG. Adhesion receptors on bone marrow stromal cells: in vivo expression of vascular cell adhesion molecule-1 by reticular cells and sinusoidal endothelium in normal and gamma-irradiated mice. Blood. 1996; 87:73–82. [PubMed: 8547679]

8. Mazo IB, et al. Hematopoietic progenitor cell rolling in bone marrow microvessels: parallel contributions by endothelial selectins and vascular cell adhesion molecule 1. J Exp Med. 1998; 188:465–474. [PubMed: 9687524]

9. Papayannopoulou T, Scadden DT. Stem-cell ecology and stem cells in motion. Blood. 2008; 111:3923–3930. [PubMed: 18398055]

10. Brakebusch C, et al. Beta1 integrin is not essential for hematopoiesis but is necessary for the T cell-dependent IgM antibody response. Immunity. 2002; 16:465–477. [PubMed: 11911830]

11. Potocnik AJ, Brakebusch C, Fassler R. Fetal and adult hematopoietic stem cells require beta1 integrin function for colonizing fetal liver, spleen, and bone marrow. Immunity. 2000; 12:653–663. [PubMed: 10894165]

12. Scott LM, Priestley GV, Papayannopoulou T. Deletion of alpha4 integrins from adult hematopoietic cells reveals roles in homeostasis, regeneration, and homing. Mol Cell Biol. 2003; 23:9349–9360. [PubMed: 14645544]

13. Bungartz G, et al. Adult murine hematopoiesis can proceed without beta1 and beta7 integrins. Blood. 2006; 108:1857–1864. [PubMed: 16735603]

14. Koni PA, et al. Conditional Vascular Cell Adhesion Molecule 1 Deletion in Mice. Impaired lymphocyte migration to bone marrow. J Exp Med. 2001; 193:741–754. [PubMed: 11257140]

15. Leuker CE, Labow M, Muller W, Wagner N. Neonatally induced inactivation of the vascular cell adhesion molecule 1 gene impairs b cell localization and t cell-dependent humoral immune response. J Exp Med. 2001; 193:755–768. [PubMed: 11257141]

16. Glodek AM, Honczarenko M, Le Y, Campbell JJ, Silberstein LE. Sustained activation of cell adhesion is a differentially regulated process in B lymphopoiesis. J Exp Med. 2003; 197:461–473. [PubMed: 12591904]

17. Dar A, et al. Chemokine receptor CXCR4-dependent internalization and resecretion of functional chemokine SDF-1 by bone marrow endothelial and stromal cells. Nat Immunol. 2005; 6:1038–1046. [PubMed: 16170318]

18. Sipkins DA, et al. In vivo imaging of specialized bone marrow endothelial microdomains for tumour engraftment. Nature. 2005; 435:969–973. [PubMed: 15959517]

19. Sugiyama T, Kohara H, Noda M, Nagasawa T. Maintenance of the hematopoietic stem cell pool by CXCL12-CXCR4 chemokine signaling in bone marrow stromal cell niches. Immunity. 2006; 25:977–988. [PubMed: 17174120]

20. Egawa T, et al. The earliest stages of b cell development require a chemokine stromal cell-derived factor/pre-b cell growth-stimulating factor. Immunity. 2001; 15:323–334. [PubMed: 11520466]

21. Nie Y, et al. The role of CXCR4 in maintaining peripheral B cell compartments and humoral immunity. J Exp Med. 2004; 200:1145–1156. [PubMed: 15520246]

22. Hargreaves DC, et al. A coordinated change in chemokine responsiveness guides plasma cell movements. J Exp Med. 2001; 194:45–56. [PubMed: 11435471]

23. Mazo IB, et al. Bone marrow is a major reservoir and site of recruitment for central memory CD8+ T cells. Immunity. 2005; 22:259–270. [PubMed: 15723813]

24. D'Apuzzo M, et al. The chemokine SDF-1, stromal cell-derived factor 1, attracts early stage B cell precursors via the chemokine receptor CXCR4. Eur J Immunol. 1997; 27:1788–1793. [PubMed: 9247593]

25. Fedyk ER, Ryyan DH, Ritterman I, Springer TA. Maturation decreases responsiveness of human bone marrow B lineage cells to stromal-derived factor 1 (SDF-1). J Leukoc Biol. 1999; 66:667–673. [PubMed: 10534124]

26. Honczarenko M, et al. SDF-1 responsiveness does not correlate with CXCR4 expression levels of developing human bone marrow B cells. Blood. 1999; 94:2990–2998. [PubMed: 10556181]

27. Galiegue S, et al. Expression of central and peripheral cannabinoid receptors in human immune tissues and leukocyte subpopulations. Eur J Biochem. 1995; 232:54–61. [PubMed: 7556170]

28. Sugiura T, Kishimoto S, Oka S, Gokoh M. Biochemistry, pharmacology and physiology of 2-arachidonoylglycerol, an endogenous cannabinoid receptor ligand. Prog Lipid Res. 2006; 45:405–446. [PubMed: 16678907]

29. Tam J, et al. The cannabinoid CB1 receptor regulates bone formation by modulating adrenergic signaling. FASEB J. 2008; 22:285–294. [PubMed: 17704191]

30. Klein TW. Cannabinoid-based drugs as anti-inflammatory therapeutics. Nat Rev Immunol. 2005; 5:400–411. [PubMed: 15864274]

31. Raghavan S, Bauer C, Mundschau G, Li Q, Fuchs E. Conditional ablation of beta1 integrin in skin. Severe defects in epidermal proliferation, basement membrane formation, and hair follicle invagination. J Cell Biol. 2000; 150:1149–1160. [PubMed: 10974002]

32. Rickert RC, Roes J, Rajewsky K. B lymphocyte-specific, Cre-mediated mutagenesis in mice. Nucleic Acids Res. 1997; 25:1317–1318. [PubMed: 9092650]

33. Horcher M, Souabni A, Busslinger M. Pax5/BSAP maintains the identity of B cells in late B lymphopoiesis. Immunity. 2001; 14:779–790. [PubMed: 11420047]

34. Tamamura H, et al. Development of specific CXCR4 inhibitors possessing high selectivity indexes as well as complete stability in serum based on an anti-HIV peptide T140. Bioorg Med Chem Lett. 2001; 11:1897–1902. [PubMed: 11459656]

35. Hoffmann R, Seidl T, Neeb M, Rolink A, Melchers F. Changes in gene expression profiles in developing B cells of murine bone marrow. Genome Res. 2002; 12:98–111. [PubMed: 11779835]

36. Kuwata N, Igarashi H, Ohmura T, Aizawa S, Sakaguchi N. Cutting edge: absence of expression of RAG1 in peritoneal B-1 cells detected by knocking into RAG1 locus with green fluorescent protein gene. J Immunol. 1999; 163:6355–6359. [PubMed: 10586023]

37. Rinaldi-Carmona M, et al. SR 144528, the first potent and selective antagonist of the CB2 cannabinoid receptor. J Pharmacol Exp Ther. 1998; 284:644–650. [PubMed: 9454810]

38. Jorda MA, et al. Hematopoietic cells expressing the peripheral cannabinoid receptor migrate in response to the endocannabinoid 2-arachidonoylglycerol. Blood. 2002; 99:2786–2793. [PubMed: 11929767]

39. Tanikawa T, Kurohane K, Imai Y. Induction of preferential chemotaxis of unstimulated B-lymphocytes by 2-arachidonoylglycerol in immunized mice. Microbiol Immunol. 2007; 51:1013–1019. [PubMed: 17951991]

40. Ziring D, et al. Formation of B and T cell subsets require the cannabinoid receptor CB2. Immunogenetics. 2006; 58:714–725. [PubMed: 16924491]

41. Woolf E, et al. Lymph node chemokines promote sustained T lymphocyte motility without triggering stable integrin adhesiveness in the absence of shear forces. Nat Immunol. 2007; 8:1076–1085. [PubMed: 17721537]

42. Oberdoerffer P, Novobrantseva TI, Rajewsky K. Expression of a targeted lambda 1 light chain gene is developmentally regulated and independent of Ig kappa rearrangements. J Exp Med. 2003; 197:1165–1172. [PubMed: 12719477]

43. Vela JL, Ait-Azzouzene D, Duong BH, Ota T, Nemazee D. Rearrangement of mouse immunoglobulin kappa deleting element recombining sequence promotes immune tolerance and lambda B cell production. Immunity. 2008; 28:161–170. [PubMed: 18261939]

44. Casellas R, et al. Contribution of receptor editing to the antibody repertoire. Science. 2001; 291:1541–1544. [PubMed: 11222858]

45. Kaminski NE, Koh WS, Yang KH, Lee M, Kessler FK. Suppression of the humoral immune response by cannabinoids is partially mediated through inhibition of adenylate cyclase by a pertussis toxin-sensitive G-protein coupled mechanism. Biochem Pharmacol. 1994; 48:1899–1908. [PubMed: 7986201]

46. Schatz AR, Koh WS, Kaminski NE. Delta 9-tetrahydrocannabinol selectively inhibits T-cell dependent humoral immune responses through direct inhibition of accessory T-cell function. Immunopharmacology. 1993; 26:129–137. [PubMed: 8282537]

47. Tokoyoda K, Egawa T, Sugiyama T, Choi BI, Nagasawa T. Cellular niches controlling B lymphocyte behavior within bone marrow during development. Immunity. 2004; 20:707–718. [PubMed: 15189736]

48. Cariappa A, et al. Perisinusoidal B cells in the bone marrow participate in T-independent responses to blood-borne microbes. Immunity. 2005; 23:397–407. [PubMed: 16226505]

49. Estalilla OC, Koo CH, Brynes RK, Medeiros LJ. Intravascular large B-cell lymphoma. A report of five cases initially diagnosed by bone marrow biopsy Am. J Clin Pathol. 1999; 112:248–255.

50. Zou YR, Kottmann AH, Kuroda M, Taniuchi I, Littman DR. Function of the chemokine receptor CXCR4 in haematopoiesis and in cerebellar development. Nature. 1998; 393:595–599. [PubMed: 9634238]
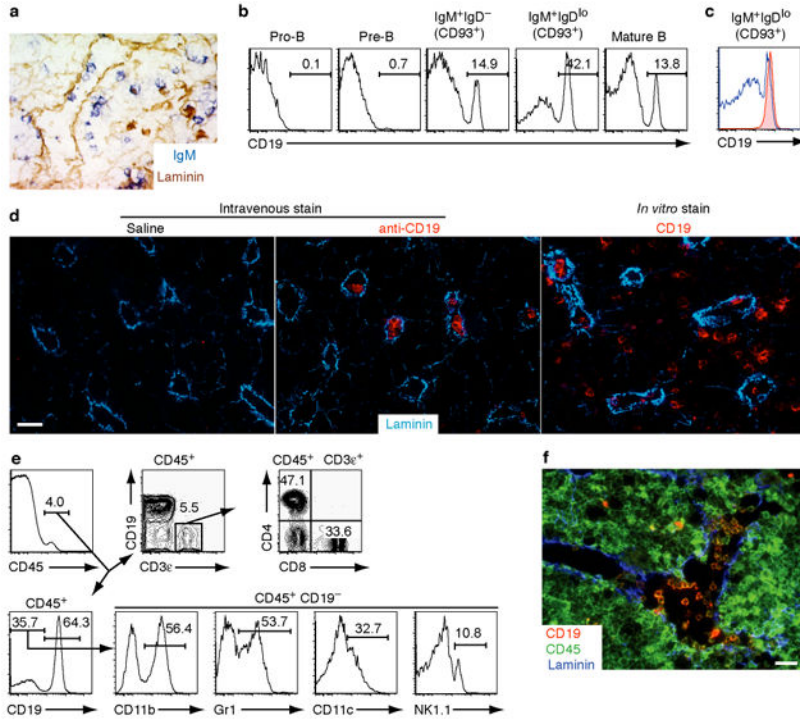
Figure 1.
In vivo labeling of B lymphocytes in BM sinusoids. (**a**) Femur section immunohistochemically stained with anti-IgM (blue) and anti-laminin (brown). Original magnification ×40. (**b,c**) Flow cytometric analysis of BM cells from a mouse injected with 1μg of anti-CD19-PE for 2 min. (**b**) Labeling of indicated BM B cell subsets. Numbers indicate % of cells in each gate. (**c**) Labeling of immature IgD^{lo} B cells in BM (blue) and peripheral blood (red). Data in **a**, **b** and **c** show one experiment and are each representative of more than 10 experiments (10 mice). (**d**) Femur or tibia sections of mice treated with saline or anti-CD19-PE, analyzed by immunofluorescence microscopy after staining with anti-laminin (blue) alone (left and middle panels) or after further *in vitro* staining with anti-CD19-PE (red) (right panel). Shown is one experiment representative of more than 10. (**e**) Flow cytometric analysis of BM cells isolated from mice injected with anti-CD45-PE for 2 min; cells were then stained *in vitro* with antibodies specific for the indicated markers. Shown is one experiment representative of two. (**f**) The femur of a mouse injected with anti-CD19-PE was analyzed by immunofluorescence microscopy after staining with anti-CD45 (green) and anti-laminin (blue). Shown is one representative image of two independent experiments (2 mice). Bar in c and f, 20μm.

Figure 2.
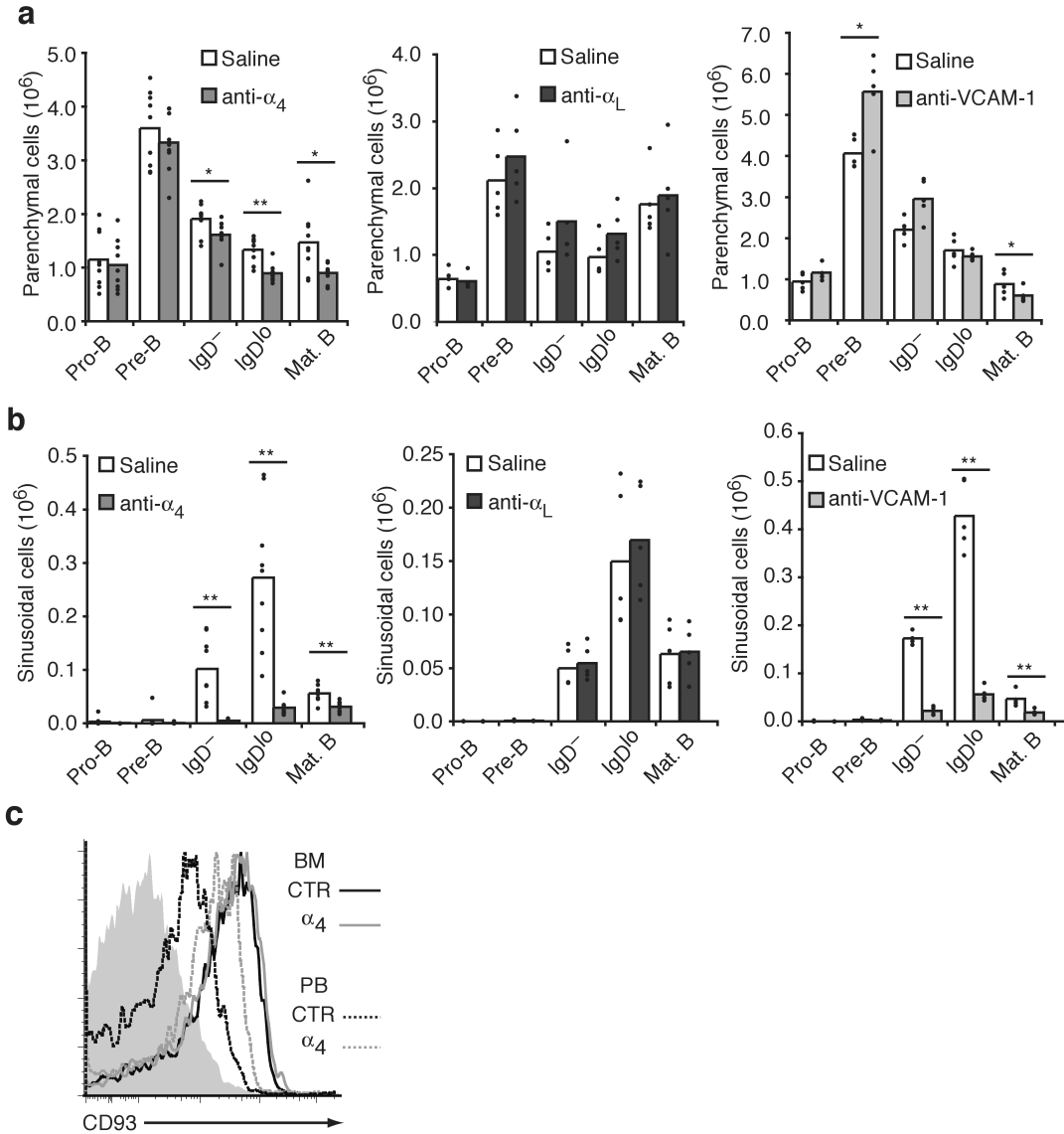α_4 and VCAM-1 promote retention of B cells inside BM sinusoids. Mice were treated with saline, anti-α_4, anti-α_L, or anti-VCAM-1 for 3 h, and with anti-CD19-PE for the last 2 min. BM B cell subsets were enumerated as parenchymal, anti-CD19-PE$^-$ (**a**) or sinusoidal, anti-CD19-PE$^+$ (**b**). Bars indicate means; circles indicate individual mice. * $P < 0.05$ and ** $P < 0.005$ by unpaired 2-tailed student t-test. (**c**) Flow cytometric anlaysis of CD93 expression on immature IgD^{lo} B cells in BM and peripheral blood (PB) of mice treated for 3 h with saline (CTR) or anti-α_4 (α_4). Mature B cells are shown for comparison (filled histogram). Data in panels **a**, **b**, and **c** are representative of three experiments (8-10 mice per experiment).
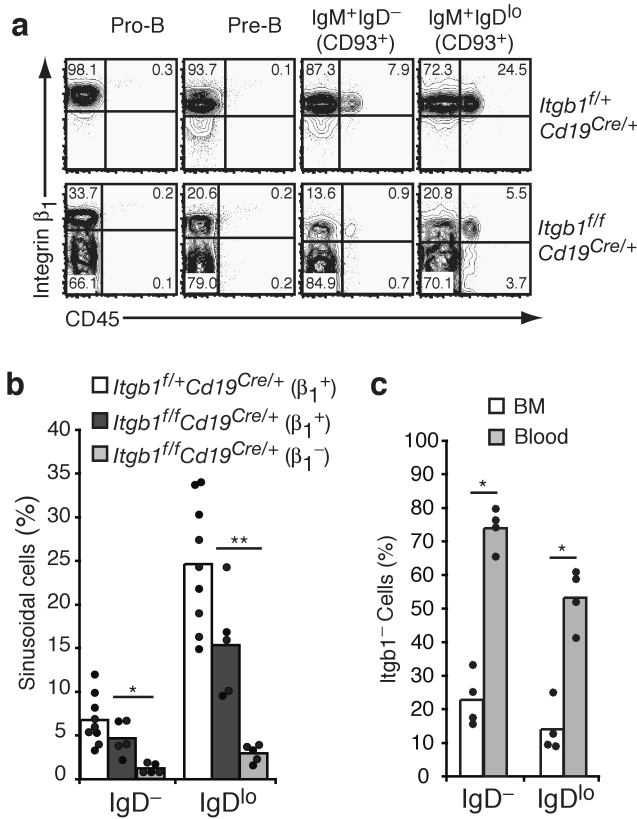
Figure 3.

β_1 integrins retain B lymphocytes inside BM sinusoids. (**a**) Flow cytometric analysis of β_1 integrin expression on BM B lineage cells in *Itgb1*$^{f/+}$Cd19-Cre$^+$ (top) or *Itgb1*$^{f/f}$Cd19-Cre$^+$ mice (bottom) treated with anti-CD45-PE for 2 min. Numbers indicate % of cells in each quadrant. (**b**) The percent of sinusoidal (CD45$^+$) cells in each B cell stage gated on β_1^+ (non-deleted) and $\beta1^-$ (deleted) cells as in the profiles in **a**. Similar findings were made with mice expressing one or two CD19-Cre alleles and these data are shown together. *n*=9 *Itgb1*$^{f/+}$Cd19-Cre$^+$ and *n*=5 *Itgb1*$^{f/f}$Cd19-Cre$^+$ mice. (**c**) The percent of β_1^- (deleted) immature B cells in the BM and blood of *Itgb1*$^{f/f}$Cd19-Cre$^+$ mice (*n*=4) was determined by flow cytometry. Data in panels **a**, **b**, and **c** are pooled from three experiments. * $P < 0.05$ and ** $P < 0.005$ by unpaired 2-tailed student t-test. In panels **b** and **c**, bars correspond to means and circles indicate individual mice.
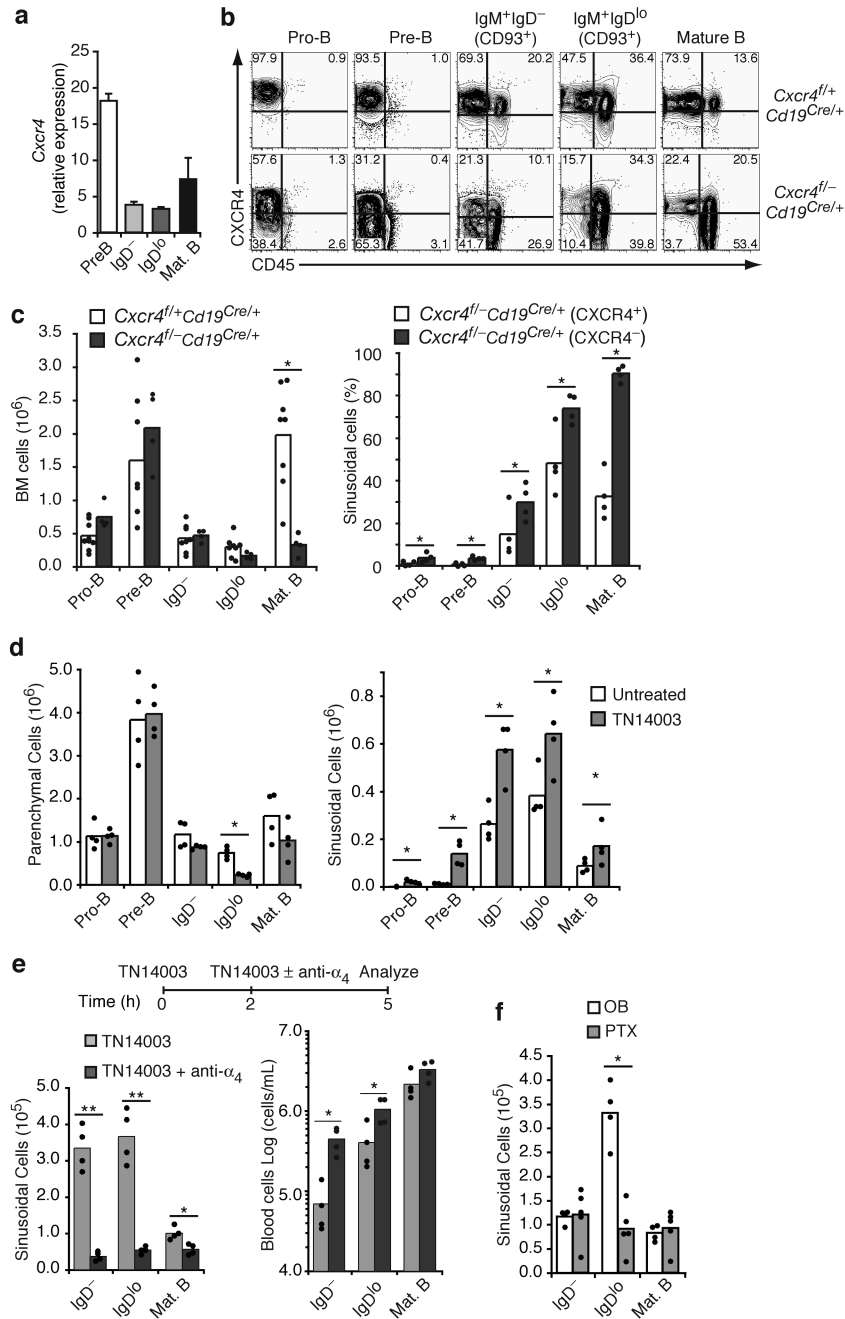
Figure 4.
CXCR4 contributes to the retention of B lineage cells in BM parenchyma but does not account for sinusoidal retention. (**a**) Purified B cell subsets were analyzed by quantitative PCR for the expression of *Cxcr4* mRNA relative to that of *Hprt1*. Data are from three independent experiments (15 mice) and bars show mean (±sd). (**b**) Flow cytometric analysis of CXCR4 expression on BM B lineage cells in *Cxcr4^{f/+}*Cd19-Cre[+] (top) and *Cxcr4^{f/−}*Cd19-Cre[+] mice (bottom). Numbers indicate % of cells in each quadrant. Data are representative of 9 mice analyzed in 3 experiments. (**c**) Total number of BM B cells (left) and percent of

sinusoidal anti-CD19-PE$^+$ B cells (right) amongst total BM B cells of the indicated phenotypes from the mice described in **b**. Data are pooled from three experiments. (**d**) Number of parenchymal (anti-CD19-PE$^-$, left) and sinusoidal (anti-CD19-PE$^+$, right) B cells of the indicated phenotypes in mice left untreated or treated for 2 h with the CXCR4 inhibitor 4F-benzoyl-TN14003. Data are representative of 9 mice analyzed in 3 experiments. (**e**) Number of sinusoidal B cells (CD19$^+$, left) and blood B cells (right) of the indicated phenotypes in mice treated with 4F-benzoyl-TN14003 for 5 h (injected at 0 and 2 h) and with saline or anti-α$_4$ for 3 h, as indicated. Data are representative of 9 mice analyzed in 3 experiments. * $P < 0.05$ and ** $P < 0.005$ by unpaired 2-tailed student t-test. (**f**) Number of sinusoidal B cells (CD19$^+$) in mice treated for 24 h with the control oligomer B (OB) subunit or with intact PTX. Data are representative of 9 mice analyzed in 3 experiments. In panels **c**, **d**, **e**, and **f**, bars correspond to means, and circles indicate individual mice.
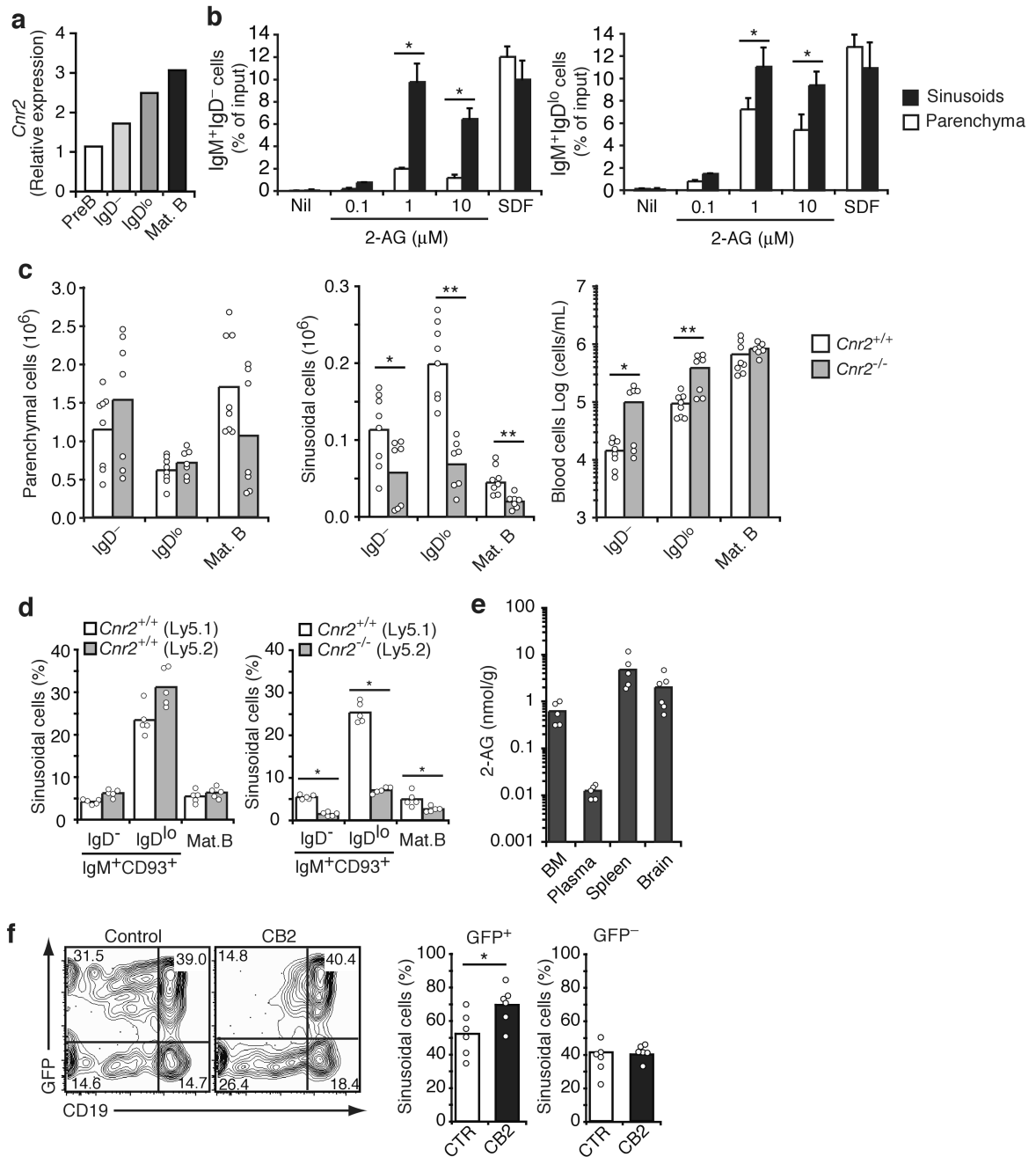
Figure 5.
CB2 is required for immature B cell lodgment in BM sinusoids. (**a**) Purified B cell subsets were analyzed by quantitative PCR for the expression of *Cnr2* mRNA relative to that of *Hprt1*. Data are representative of 2 experiments (2 mice). (**b**) Migration of immature B cells to 2-AG. BM cells from anti-CD19-PE treated mice were placed in Transwells, and migration of immature IgM⁺D⁻ and IgM⁺D^lo B cells towards the indicated concentrations of 2-AG or SDF-1 (0.3 μg/ml) was measured. Data are representative of 10 experiments (10 mice). (**c**) Number of parenchymal (anti-CD19-PE⁻, left) and sinusoidal (anti-CD19-PE⁺,

middle) BM B cells and blood B cells (right) of the indicated types in $Cnr2^{+/+}$ ($n=8$) and $Cnr2^{-/-}$ ($n=7$) mice. Data are pooled from 3 experiments. (**d**) Percent of in vivo anti-CD19-PE labeled cells of the indicated phenotypes in BM of mice reconstituted with a mix of Ly5.1$^+Cnr2^{+/+}$ and Ly5.2$^+Cnr2^{+/+}$ or Ly5.1$^+Cnr2^{+/+}$ and Ly5.2$^+Cnr2^{-/-}$ BM cells. Data are representative of 4 experiments (5 mice of each group). (**e**) 2-AG concentration in the indicated tissues, determined by mass spectrometry. Data are pooled from 3 experiments (4-10 mice). (**f**) Left panels show flow cytometric analysis of BM from mice that had received B cells transduced with retroviruses encoding GFP alone (CTR), or CB2 and GFP (CB2), and that were injected with anti-CD19-PE 2 minutes prior to analysis. Numbers indicate % of cells in each quadrant. Right panels show percent of transferred GFP$^+$ and GFP$^-$ cells in BM sinusoids (anti-CD19-PE$^+$). Data are pooled from 3 experiments (6 mice). In panels **b**, **c**, **d**, **e**, and **f**, bars indicate means and circles indicate individual mice.
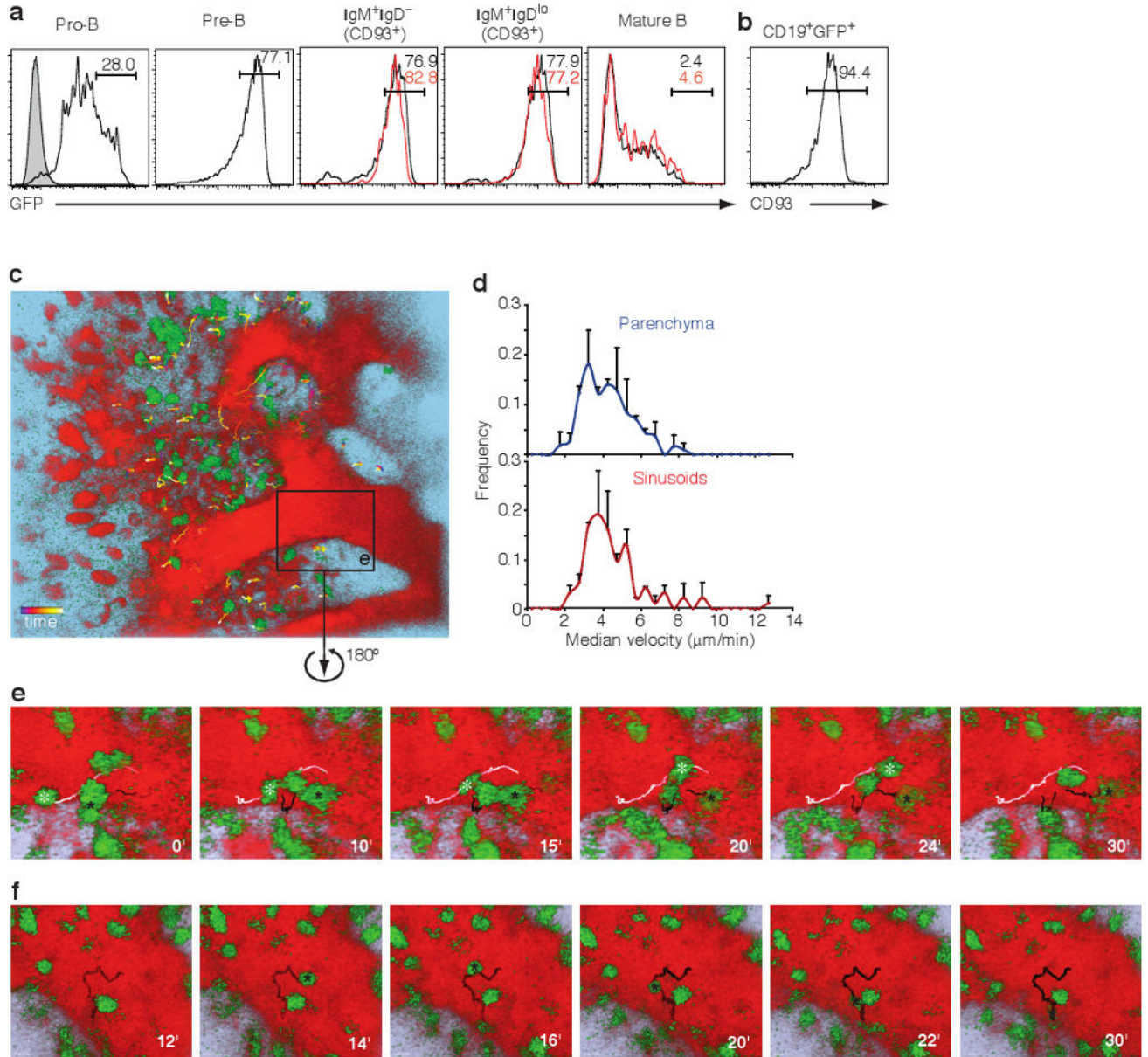
Figure 6.
Migration dynamics of immature B cells in BM sinusoids. (**a**) Flow cytometric analysis of $Rag1^{GFP/+}$ BM from mice treated for 2 minutes with anti-CD19-PE. Histograms show GFP intensity of anti-CD19-PE$^-$ (black lines) and anti-CD19-PE$^+$ cells (red lines). Shaded histogram in left panel shows B220$^-$ cells. (**b**) Flow cytometric analysis of CD93 expression on anti-CD19-PE$^+$ GFP$^+$ sinusoidal B cells. Data in **a** and **b** are representative of 3 experiments (3 mice). (**c**) Image showing the migratory pattern in parenchyma and sinusoids of developing B cells. Box indicates region shown in **e** after *z* rotation of 180°. Tracks of several motile cells are shown. Tracks are highlighted in a time scale (bottom left) with the earliest track times in blue and the latest in white. Due to the depth of the projected image, tracks are sometimes partially obscured. See also Supplementary Movie 1. (**d**) Median

velocities of parenchymal and sinusoidal GFP^{+} cells. Data are from two movies (2 mice). 60 parenchymal and 50 sinusoidal cells were tracked in each movie. Error bars indicate s.d.. (**e**) Timelapse images showing GFP[+] cell entry and migration within a BM sinusoid. A cell migrating within the sinusoid is highlighted by a white asterisk and track, and a cell that enters the sinusoid from the parenchyma is highlighted by a black asterisk and track. (**f**) Time lapse images showing a GFP[+] cell being captured from flow and beginning to migrate. The cell is highlighted by a black asterisk and track. See also Supplementary Movie 2. Numbers indicate time in minutes.
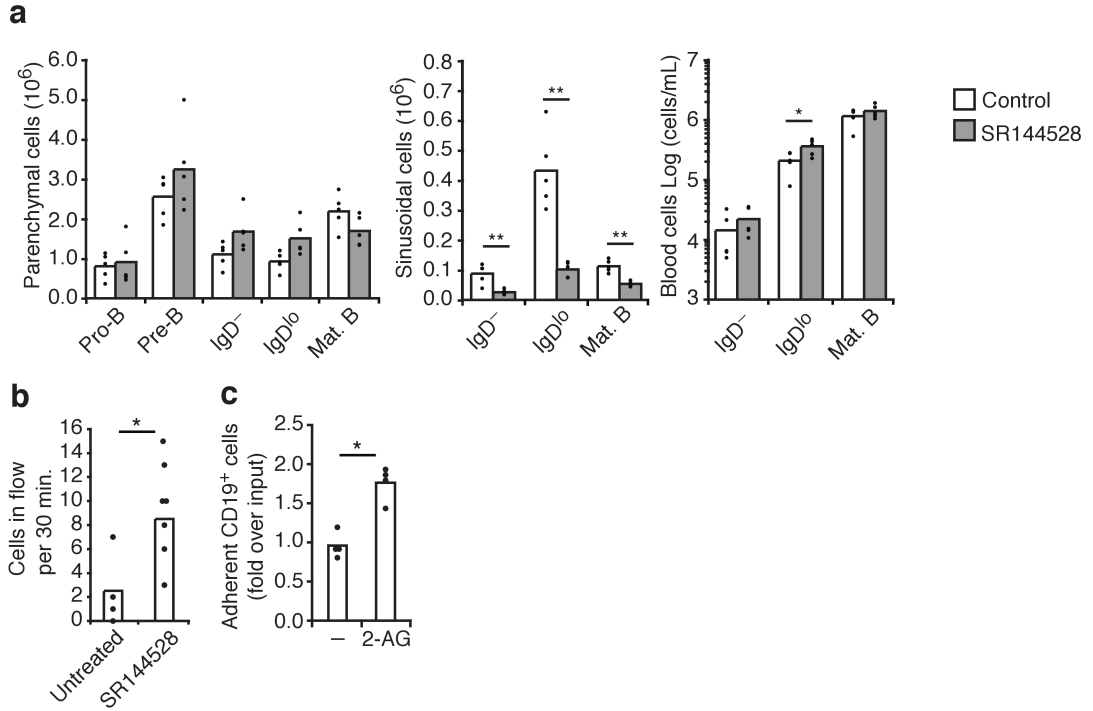
Figure 7.
Constitutive requirement for CB2 to retain B cells in BM sinusoids. (**a**) Displacement of immature B cells from BM sinusoids following 3 h treatment with a CB2-specific antagonist SR144528., but not with control treatment (carrier, 0.1% ethanol in saline) Number of parenchymal (anti-CD19-PE⁻, left) and sinusoidal (anti-CD19-PE⁺, middle) BM B cells <u>and of blood B cells (right)</u> of the indicated phenotypes are shown. Data are representative of at least 5 experiments (5 mice in each experimental condition). (**b**) $Rag1^{GFP/+}$ B cells in fluid phase within BM sinusoids were detected by intravital 2-photon microscopy. Data are shown as number of events per 30 min imaging period before (untreated) or after SR144528 treatment. Data are representative of 2 experiments (2 mice). (**c**) BM B cells from mice injected with anti-CD19-PE were passed through VCAM-1 coated flow chambers at ~1 dyne/cm^2 of shear in the absence (–) or presence of 2-AG for 30 min. At the end of each time interval, fluorescent images of the flow chamber were captured and numbers of bound anti-CD19-PE⁺ and anti-CD19-PE⁻ cells were enumerated. The change in the percent of CD19⁺ cells in the bound fraction compared to the input is shown. Bars indicate means of four independent experiments (circles). * $P < 0.05$ and ** $P < 0.005$, respectively (student's t-test).
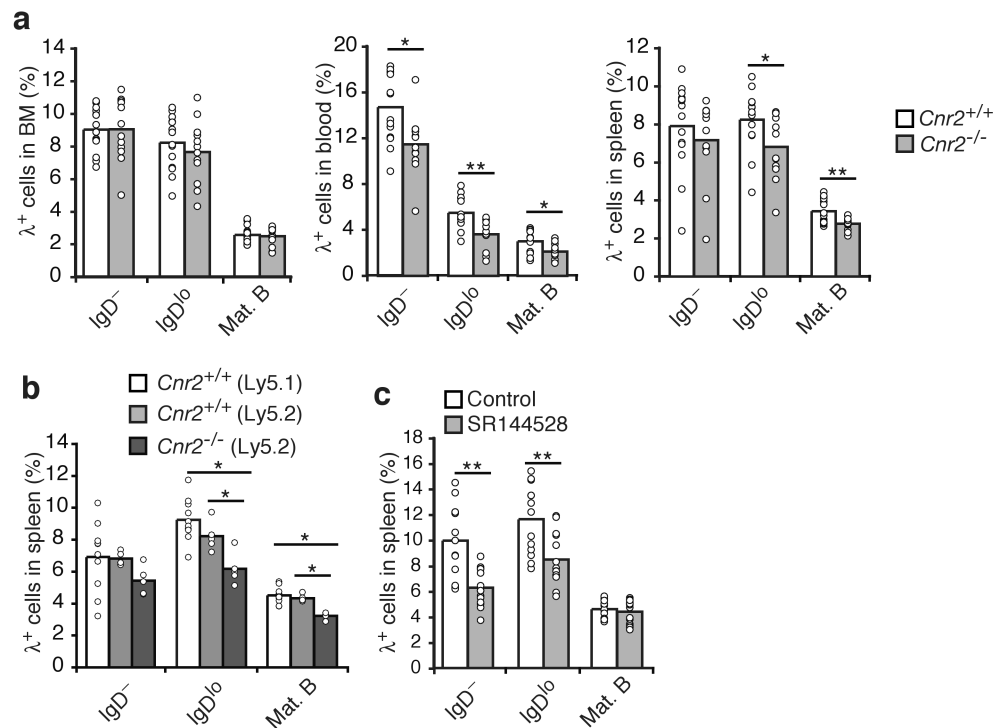
Figure 8.
Decreased frequency of Igλ⁺ B cells in CB2-deficient mice. Percent of Igλ⁺ immature and mature B cells in total BM, blood and spleen of *Cnr2*⁺/⁺ (*n*=14) and *Cnr2*⁻/⁻ (*n*=12) mice (**a**) or in spleen of chimeric mice reconstituted with a mix of Ly5.1⁺*Cnr2*⁺/⁺ and Ly5.2⁺*Cnr2*⁺/⁺ (*n*=5) or Ly5.1⁺*Cnr2*⁺/⁺ and Ly5.2⁺*Cnr2*⁻/⁻ (*n*=4) BM cells (**b**) or in mice treated with carrier (control, *n*=13) or SR144528 (*n*=14) (**c**). a and b each represent pooled data from 3 independent experiments. In c mice were treated for 6 days (one experiment) or 9 days (two experiments) with similar results and the data were pooled. Bars indicate means; circles indicate individual mice. * $P < 0.05$ and **$P < 0.005$, respectively (student's t-test).